Structure and electronic properties of Thue-Morse lattices

Zheming Cheng, Robert Savit, and R. Merlin
Department of Physics, University of Michigan, Ann Arbor, Michigan 48109-1120
(Received 10 August 1987)

We study a one-dimensional system which is neither periodic, quasiperiodic, nor random. We find that the structure factor of this system consists of a set of peaks whose heights scale with L, the length of the chain, according to $L^{\alpha(k)}$. We show that for $k<\frac{1}{2}$, $\alpha(k)\leq\alpha(\frac{1}{3})=\ln 3/\ln 2$, so that all of the peaks vanish relative to the peak at the center of the Brillouin zone (which is associated with the periodicity of the underlying lattice) as the system grows. We also prove a number of other properties of these exponents. We discuss the energy spectrum of this system for both weak and strong potentials. We show how the gaps in the two limits are related, and we argue that, despite the expectations of naive perturbation theory, gaps persist in the $L\rightarrow\infty$ limit.

I. INTRODUCTION

One-dimensional Schrödinger equations with quasiperiodic potentials have been extensively studied in the past several years.[1] More recently, much attention has focused on potentials derived from the Fibonacci sequence.[2] Aside from their purely theoretical interest, a number of these latter studies were motivated in part by the discovery of metallic alloys manifesting icosahedral symmetry,[3] and the interpretation of these findings in terms of the quasicrystalline state,[4] as well as the experimental realization of Fibonacci superlattices.[5]

The rich and intriguing properties of these structures suggests the utility of studying systems based on more general sequences. In this paper, we will study the structure factor and electronic properties of a one-dimensional system which is based on a sequence that is neither periodic, quasiperiodic, nor random. The system we will consider is called the Thue-Morse lattice.[6] The associated sequence is a generalization of quasiperiodic sequences, in that, unlike the latter, the Thue-Morse sequence cannot be characterized by a finite set of irrational numbers. In some sense, an infinite number of irrational periods are present in this case. Like quasiperiodic systems, the Thue-Morse structure factor is composed of a sequence of δ-function peaks. However, unlike normal quasiperiodic systems, these peaks do not scale like L^2, where L is the length of the system. In fact, they have a very complicated scaling structure, with different sets of peaks scaling with different exponents. Similarly, the electronic structure, which we have calculated in perturbation theory (and which agrees surprisingly well with nonperturbative numerical computations), is quite complex and interesting.

The Thue-Morse chain of order N is a sequence of length 2^N composed of two symbols a and b. The chain of order $N+1$ is generated from the chain of order N by making the following substitution for each symbol in the order N chain:

$$a\rightarrow\sigma(a)=ab,\quad b\rightarrow\sigma(b)=ba\ . \tag{1}$$

If we take as the chain of order zero the sequence a, then the chain of order 5, for example, is given by

$$\sigma^5(a)=abbabaabbaabbabbabaabbabbaabbabaab\ . \tag{2}$$

Using (1), it is not difficult to see that

$$\sigma^{n+1}(a)=\sigma^n(a)\bar{\sigma}^n(a)\ , \tag{3}$$

where $\bar{\sigma}^n(a)$ is the complement of $\sigma^n(a)$ obtained by interchanging a and b in $\sigma^n(a)$.

Another interesting and useful relation follows from the definition (1) of the chain. If we let $a=1$ and $b=-1$, then the symbol at the nth position of the Thue-Morse chain (assuming the zeroth-order chain is just 1) is given by

$$f(n)=\exp\left[i\pi\sum_j c_j\right]\ , \tag{4}$$

where $(\cdots c_j c_{j-1}\cdots c_2 c_1)$ is the binary representation of the integer n.

The rest of this paper is organized as follows. In Sec. II we will discuss the structure factor of the Thue-Morse lattice. We will derive a formula for the intensity as a function of both the wave vector k and the size of the system. We will show that the intensity at different wave vectors scales with the size of the system in different ways. The scaling is determined by an exponent $\alpha(k)$. We will show that for almost all frequencies, $\alpha(k)$ exists and is zero. Those frequencies for which $\alpha(k)$ is nonzero can be grouped into classes, each member of a given class having the same value of α. The largest value of α [aside from the trivial case of $\alpha(k=\frac{1}{2})=2$ which is associated with the center of the Brillouin zone and just reflects the periodicity of the underlying lattice] occurs for the class of frequencies which includes $k=\frac{1}{3}$, and we find $\alpha(\frac{1}{3})=\ln 3/\ln 2$. In Sec. III we turn to a discussion of the electronic properties within the tight-binding formalism. We first discuss the limit of weak potentials of the Thue-Morse form and compute the energy spectrum of a finite system using second-order perturbation theory. Next, we study the model in the limit of very strong potentials. By considering both the weak- and strong-potential limits,

we are able to produce a scenario for the behavior of the energy gaps as a function of the potential strength. Finally, in Sec. III, we address the behavior of the electronic spectrum in the thermodynamic limit for fixed potential strength. We suggest that for any small but finite potential, there are nonzero energy gaps even in the limit of an infinite system. This suggestion is contrary to the predictions of naive second-order perturbation theory, but we argue that such an approach is inapplicable in this limit. All of our conclusions and results are consistent with the results of Axel *et al.*[6] who computed the band structure numerically in a tight-binding model. Section IV consists of a summary of our results and their implications, as well as a brief discussion of remaining questions.

II. STRUCTURE FACTOR

A. Derivation of the structure factor

Consider the chain defined by the function $f(n)$ in Eq. (4). The two possible values a and b associated with the sites of the chain [in the representation of Eq. (4), $a=1$, $b=-1$] can be considered to label two different kinds of atoms or diffraction centers with different scattering factors.

It is straightforward to derive an expression for the intensity of the Fourier transform of the Thue-Morse chain defined above. Consider the chain $\sigma_N(a)$ of 2^N elements with $a=1$ and $b=-1$. Then,

$$I_{N+1}(k)=\left|\sum_{n=0}^{2^{N+1}-1} f(n)e^{2\pi ink}\right|^2=\left|\sum_{n=0}^{2^N-1} f(n)e^{2\pi ink}+\sum_{n=2^N}^{2^{N+1}-1} f(n)e^{2\pi ink}\right|^2 . \tag{5}$$

Using the easily proven relation

$$f(2^N+n)=-f(n) , \tag{6}$$

(5) becomes

$$I_{N+1}(k)=I_N(k)\,|\,1-\exp(2\pi ik2^N)\,|^2 . \tag{7}$$

Equation (7) is a simple recursion relation for $I_N(k)$ which is easily solved to yield

$$I_N(k)=2^{2N}\sum_{n=0}^{N-1}\sin^2(\pi 2^n k) . \tag{8}$$

For the purposes of deriving properties of $I_N(k)$, two other forms of Eq. (8) will be useful. First, (8) can easily be rewritten as

$$I_N(k)=2^{2N}\sum_{n=1}^{N}\sin^2(\pi k_n/2),\quad 0\le k_n\le 1 \tag{9}$$

and

$$k_{n+1}=\begin{cases}2k_n, & 0\le k_n\le\frac{1}{2}\\ 2-2k_n, & \frac{1}{2}\le k_n\le 1\end{cases} , \tag{10}$$

with $k_1=2k$. Another useful form of (8) can be obtained by defining $\varphi_n=2^n k \pmod 1$. In this case (9) and (10) can be expressed as

$$I_N(k)=2^{2N}\prod_{n=0}^{N-1}\sin^2(\pi\varphi_n),\quad 0\le\varphi_n\le 1 , \tag{11}$$

$$\varphi_{n+1}=2\varphi_n \pmod 1,\quad 0\le\varphi_n\le 1 , \tag{12}$$

with $\varphi_0=k$. The recursion relation (10) is a special case of the well-studied Kac map,[7] some general results of which we shall use in the next subsection.

Equation (10) can also be understood in another way which will be very useful. Let

$$0.c_1(n)c_2(n)c_3(n)\ldots \tag{13}$$

be the binary representation of k_n, where $c_i(n)=0$ or 1. Then Eq. (10) becomes

$$\begin{aligned} k_{n+1}&=0.c_2(n)c_3(n)c_4(n)\ldots, \quad \text{if } c_1(n)=0 ,\\ k_{n+1}&=0.\bar{c}_2(n)\bar{c}_3(n)\bar{c}_4(n)\ldots, \quad \text{if } c_1(n)=1 ,\end{aligned} \tag{14}$$

where $\bar{c}_j(n)$ is the complement of $c_j(n)$. Thus (14) is either a shift or shift combined with complement operation.

In Fig. 1 we show a plot of $I_N(k)$, the structure factor for the Thue-Morse chain defined in Eq. (4) with $N=10$ (i.e., with 1024 elements). Plots of $I_N(k)$ for larger values of N are qualitatively similar but have more peaks. Note that the peaks are larger and more concentrated around the frequencies $\frac{1}{3}$ and $\frac{1}{6}$. The positions and intensities of major peaks are apparently more complex than in the periodic or quasiperiodic case. Furthermore, a comparison of plots of $I_N(k)$ for different values of N suggests that the sizes of different peaks scale differently with the size of the system, unlike the case of periodic and quasiperiodic systems. We turn now to a discussion of the scaling properties and relative heights of the peaks in the spectrum $I_N(k)$.

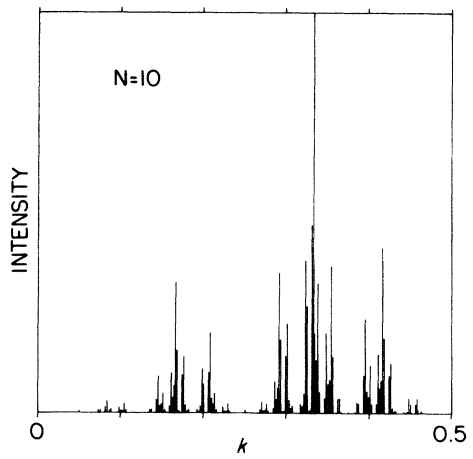

FIG. 1. Structure factor of a Thue-Morse chain with $N=10$.

B. Scaling exponents of the structure factor

In the usual periodic and quasiperiodic systems, the intensities of the peaks in the structure factor scale like L^2, where L is the size of the system. This result holds for the entire structure factor, independent of k, so that the relative intensities of the peaks in the spectrum are independent of L. But this is not true in our case as is most easily seen by referring to Eq. (8). The first factor in this expression is just L^2, where $L=2^N$ is the length of the system labeled by N. This is the scaling factor we naively expect from our experience with periodic and quasiperiodic systems. However, as we show below, the product in Eq. (8) tends to zero for almost all wave vectors, and it tends to zero at different rates for different k's. Therefore, in general, the exponents defining the scaling of $I_N(k)$ with the size of the system are different for different wave vectors. It is also the case that there are wave vectors for which no well-defined scaling exponent exists. An example will be given below.

Let us suppose then that, in general, $I_N(k)$ scales with the size of the system like

$$I_N(k)=L^{\alpha_N(k)}, \tag{15}$$

where $L=2^N$, and $\alpha_N(k)$ is the effective scaling exponent at wave vector k for a system of size 2^N. From Eq. (11) we see that

$$\alpha_N(k)=2\left[1-\frac{1}{N\ln 2}\sum_{n=0}^{N-1}\ln[\sin(\pi\varphi_n)]\right]. \tag{16}$$

Let us consider the large-N limit of $\alpha_N(k)$ defined as

$$\alpha(k)=\lim_{N\to\infty}\alpha_N(k). \tag{17}$$

We will now prove five important properties of $\alpha(k)$.

1. *For almost every k in $[0,\frac{1}{2}]$, $\alpha(k)=0$*

Proof. It is well known[7] that the map (12) has the property that for almost every $\varphi_0=k$, φ_n is uniformly distributed in [0,1] in the limit $n\to\infty$. Therefore, for almost every k we can change the sum in Eq. (16) into an integral in the limit $N\to\infty$. Thus

$$\alpha(k)=\lim_{N\to\infty}2\left[1-\frac{1}{N\ln 2}\sum_{n=0}^{N-1}\ln[\sin(\pi\varphi_n)]\right]$$

$$=2-\frac{2}{\ln 2}\int_0^1\ln[\sin(\pi\tau)]d\tau=0 \tag{18}$$

Q.E.D.

2. *$\alpha(\frac{1}{3})=\ln 3/\ln 2$ is the largest scaling exponent*

Proof. It is easy to calculate $\alpha(\frac{1}{3})$ once we realize that $k=\frac{1}{3}$ (i.e., $k_1=k_2=\cdots=k_N=\frac{2}{3}$) is a fixed point of Eq. (10). Thus all the terms in the sum on the right-hand side of Eq. (16) are the same. Since $\sin^2(\pi/3)=\frac{3}{4}$, $\alpha(\frac{1}{3})=\ln 3/\ln 2$.

Now we prove that $\alpha(\frac{1}{3})$ is the largest scaling exponent. Equation (9) reads

$$I_N(k)=2^{2N}\sin^2(\pi k_1/2)\sin^2(\pi k_2/2)\cdots\sin^2(\pi k_N/2). \tag{19}$$

Since all $k_j=\frac{2}{3}$, each factor of $\sin^2$ in this expression is the same. Now, consider any wave vector k' other than $\frac{1}{3}$. Using Eq. (9) we will generate another sequence of wave vectors k_j'. Since $\sin(\beta)$ is a monotonically increasing function of β for $0\le\beta\le\pi/2$, the smaller k_i is, the smaller will be the ith factor in (19). Suppose that for some i, k_i' is larger than $\frac{2}{3}$. We may write $k_i'=\frac{2}{3}+\delta$, with $0<\delta<\frac{1}{3}$. Then, using (10), we have $k_{i+1}'=\frac{2}{3}-2\delta$, which is less than $\frac{2}{3}$. But,

$$\sin^2(\pi k_i'/2)\sin^2(\pi k_{i+1}'/2)$$

$$=\sin^2[\pi(\tfrac{2}{3}+\delta)/2]\sin^2[\pi(\tfrac{2}{3}-2\delta)/2]$$

$$<\sin^2[\pi(\tfrac{2}{3}+\delta)/2]\sin^2[\pi(\tfrac{2}{3}-\delta)/2]$$

$$<\tfrac{9}{16}=\sin^4[\pi(\tfrac{2}{3})/2]. \tag{20}$$

That is, if a k_i' is generated which is greater than $\frac{2}{3}$, k_{i+1}' will be sufficiently small so that inequality (20) holds. Thus if the limits exist,

$$\lim_{N\to\infty}I_N(k')/I_N(\tfrac{1}{3})\le 1,$$

and

$$\alpha(k')\le\alpha(\tfrac{1}{3})$$

Q.E.D.

3. *If k' and k'' are two wave vectors such that $\Delta\equiv k'-k''$ has a finite-length binary representation, then $\alpha(k')=\alpha(k'')$, if they exist*

Proof. If Δ has a finite-length binary representation, then there exists a p such that for all $j>p$, $k_j'=k_j''$ [i.e., after a finite number of iterations of Eq. (10), k_j' and k_j'' will be equal forever]. This is apparent if we refer to Eq. (14), which is just a binary version of Eq. (10). Since each iteration shifts the sequence of binary digits on space to the left, and since $0\le k_j\le 1$, it is clear that if Δ has a finite-length binary representation, then eventually the digits to the right of the decimal point will form the same sequence for k_j' and k_j''. But changing a finite number of factors in Eq. (9), or, what is the same thing, changing a finite number of terms in Eq. (16) will not change the $N\to\infty$ limit of α_N, so that $\alpha(k')=\alpha(k'')$. Q.E.D.

4. *For every rational wave vector k, $\alpha(k)$ exists*

Proof. Using (14), the binary form of the recursion relation, it is clear that for any rational k, the sequence k_j will reach a limit cycle after a finite number of iterations. The length of the limit cycle is the same as the length of the digital cycle of k in binary form. Thus $\alpha(k)$ exists and can be calculated. Q.E.D.

5. *There are values of k for which no well-defined scaling exponent exists*

Example. Consider a wave vector (irrational) defined by a binary string which consists of alternating sequences

taken from the binary representation of two rational numbers. For example,

$$k=0.100101000000000101010101010101010\ldots$$

the first digit to the right of the decimal is the first digit of the binary representation of $\frac{1}{3}$. The next 2 digits are from the binary representation of 0. The following 4 digits come from the representation of $\frac{1}{3}$, followed by 8 digits from 0, 16 digits from $\frac{1}{3}$, etc. It is easy to see that for this sequence $\alpha_N(k)$ does not approach any well-defined limit in the sense of Eq. (17).

These results tell us a good deal about the structure of Thue-Morse lattices. First, property 3 offers a natural way of classifying wave vectors according to their scaling exponents. Furthermore, using property 4, it is easy to see that $\alpha(k=0)=-\infty$, so that the values of the scaling exponents can range from $-\infty$ to $\alpha(\frac{1}{3})=\ln 3/\ln 2$. Moreover, it is not difficult to show that $\alpha(k)$ for rational k is dense in the interval $(-\infty, \ln 3/\ln 2]$, so that for every number in this interval, there is some wave vector whose scaling exponent is equal to that number.

As stated in property 1, for most k's, the intensity is unaffected by changes in the size of the system. $\alpha(k)>0$ only for a subset of wave vectors. But even for these k's, $I_N(k)$ does not increase as rapidly as the peaks in periodic or quasiperiodic systems do. In a real discrete physical system, there will be a (trivial) peak in the structure factor corresponding to the periodicity of the underlying lattice ($k=\frac{1}{2}$). The intensity in this peak will increase like L^2, and so relative to this peak all the nontrivial peaks associated with the Thue-Morse structure will diminish.

Nevertheless, the structure of $I_N(k)$ is complex and interesting. Neglecting the trivial peak, we see that for very large systems, only those peaks related to $k=\frac{1}{3}$ by property 3 will persist. It is interesting to examine the region around one of these peaks, say, the one at $k=\frac{1}{3}$, to see how the intensity in nearby frequencies behaves as N increases. Because of property 3, for large enough N, we will always be able to find another peak arbitrarily close to $k=\frac{1}{3}$, much smaller in magnitude, but whose scaling exponent is $\alpha(k=\frac{1}{3})$. Thus in some sense each peak in a finite system foreshadows the existence of a group of nearby peaks which become increasingly dense as N increases and which scale with the same exponent.

III. ELECTRONIC PROPERTIES

In this section we turn our attention to the behavior of nonrelativistic particles (electrons) in a potential with the structure of the Thue-Morse chain. Specifically, we consider a one-dimensional potential of the form

$$V_N(n)=\begin{cases} f(n), & 0<n<2^N \\ \infty, & \text{otherwise}, \end{cases} \tag{21}$$

where $f(n)$ is defined in Eq. (4). The tight-binding version of the Schrödinger equation which we will study is

$$\psi(n+1)+\psi(n-1)+[-\lambda V_N(n)+E-2]\psi(n)=0\ , \tag{22}$$

where E is the energy eigenvalue, ψ is the wave function, and λ is the strength of the potential in Eq. (21). Also associated with the solution of Eq. (22) are boundary conditions, and fixed-edge boundary conditions are implicit in the form of the potential (21).

We will use (22) to compute the positions and sizes of the gaps in the energy spectrum. In particular, we will study (22) in both the weak- and strong-perturbation limits. We will find that certain qualitative features of the spectrum are the same in both limits, and we will discuss the reasons for the similarities. We will also discuss some aspects of the delicate $N\to\infty$ limit.

A. Weak-perturbation limit

Consider Eq. (22).[8] Its Fourier transform is

$$\sum_k \{[E_0(k)-E]\delta_{kq}+\lambda\tilde{V}_N(k-q)\}\tilde{\psi}(k)=0\ , \tag{23}$$

where $E_0(k)=4\sin^2(\pi k)$, δ is a Kronecker delta function, and $\tilde{V}$ and $\tilde{\psi}$ are the Fourier components of V and ψ, respectively. The eigenvalues are determined by the secular equation

$$\mathrm{Det}\{[E_0(k)-E]\delta_{kq}+\lambda\tilde{V}_N(k-q)\}=0\ . \tag{24}$$

For small enough λ, one can, in principle, expand (24) as a power series in λ and obtain good approximations for E from the leading terms in the expansion. However, if λ is small, but not too small, the typical size of the perturbation may be larger than the energy difference between k-vector eigenstates that can be connected by nonzero values of $\tilde{V}_N(k)$. Those states should then be regarded as degenerate or nearly degenerate, and the calculation, in general, involves the exact evaluation of the determinants of a number of matrices, the size of each matrix being proportional to the number of states which are degenerate or nearly degenerate. In our case, the spectrum of $V(n)$ becomes increasingly dense as L, the size of the system, increases. Thus the typical separation between states that can be connected by nonzero $\tilde{V}_N(k)$ is of order $L^{-1}=2^{-N}$. A tractable weak-perturbation calculation can, therefore, only be carried out if $\lambda\lesssim L^{-1}$. (Note that this is qualitatively different than the periodic case in which $\tilde{V}_N(k)$ is nonzero for only a few values of k, regardless of N.)

If $\lambda\lesssim L^{-1}$ the shift in energy for each value of k is primarily due to the mixing of the unperturbed states of wave vectors k and $-k$, as is usual in second-order perturbation theory. In this case we have

$$E(k)=E_0(k)\pm\lambda\,|\,\tilde{V}_N(k)\,|\ . \tag{25}$$

Thus in this weak-perturbation limit, each peak in the structure factor corresponds to a (small) gap in the band structure.

Now (25) is formally similar to the result obtained for a system subject to a periodic potential. But in our case, the calculation leading to (25) can hardly be taken seriously for large systems, since it requires $\lambda\lesssim L^{-1}$, rather than $\lambda\lesssim 1$ as required for the periodic case. Nevertheless, this calculation, when combined with the results of a strong-perturbation calculation, can give us a good deal

of insight into the general energy spectrum of the Thue-Morse chain. In fact, if we look at Fig. 1 and compare the results computed using this $\tilde{V}_N(k)$ in (25) with the numerical calculation of Axel *et al.*[6] for the Thue-Morse phonon spectrum, we see that the correspondence between peaks in the structure factor and energy gaps in the excitation spectrum is very close. (See also the discussion in Sec. III B.) This suggests that Eq. (25) may be qualitatively correct for a much larger range of λ than its derivation implies. Indeed, as we shall now discuss, the sizes and positions of the gaps in the large-λ limit are closely correlated with the sizes and positions of the peaks of $\tilde{V}_N(k)$.

B. Strong-perturbation limit

We turn now to a discussion of the energy spectrum for very large λ. Using (22), the discretized, tight-binding version of the Schrödinger equation, we can develop a systematic expansion in powers of λ^{-1} for the energy eigenvalues. Although the calculational details become rather complicated after second order, we can gain considerable insight into the robustness of certain features of the band structure over a range of values of λ.

In the limit of extremely large λ, the couplings between regions of unit length (the distance over which the potential varies) in the chain become relatively unimportant, and the energy spectrum is that of a collection of independent particles, each sitting in its own local potential. Hence, there are two energy eigenvalues given by $E=\lambda V_N(n)+2\approx\pm\lambda$, each of which is $L/2$-fold degenerate, where $L=2^N$ is the number of sites in the chain.

The first nontrivial correction to this result comes when we consider the fact that the electron's wave function can extend over more than one unit interval in the Thue-Morse potential. We thus consider the first two terms in (22) as perturbations on the single-site states. In general, the energy eigenvalues of (22) are just the solutions of the determinental equation

$$\text{Det}\begin{bmatrix} -\lambda V_N(1)+E-2 & 1 & 0 & \cdots & 0 \\ 1 & -\lambda V_N(2)+E-2 & 1 & \cdots & \vdots \\ 0 & 1 & & \ddots & \vdots \\ \vdots & 0 & & & 1 \\ 0 & \cdots & \cdots & 1 & -\lambda V_N(2^N)+E-2 \end{bmatrix}=0 . \tag{26}$$

Keeping only the leading terms in λ, we obtain the lowest-order result quoted above. To most easily see the effects of the next-order correction, we rearrange the matrix such that all the diagonal elements with $V_N(n)=+1$ appear in the upper left quadrant, while all the diagonal elements with $V_N(n)=-1$ appear in the lower right quadrant. In addition we keep the elements in ascending order of the arguments n of $V_N(n)$. The result is that (26) becomes

$$\text{Det}\begin{bmatrix} A & B \\ B^T & C \end{bmatrix}=0 , \tag{27}$$

where

$$A=\begin{bmatrix} e(i_1) & \varphi(i_1,i_2) & \cdots & \cdots & 0 \\ \varphi(i_1,i_2) & e(i_2) & \cdots & \cdots & \vdots \\ \vdots & \vdots & & \ddots & \vdots \\ \vdots & \vdots & & & \varphi(i_{m-1},i_m) \\ 0 & \cdots & \cdots & \varphi(i_{m-1},i_m) & e(i_m) \end{bmatrix},$$

$$C=\begin{bmatrix} e(j_1) & \varphi(j_1,j_2) & \cdots & \cdots & 0 \\ \varphi(j_1,j_2) & e(j_2) & \cdots & \cdots & \vdots \\ \vdots & \vdots & & \ddots & \vdots \\ \vdots & \vdots & & & \varphi(j_{m-1},j_m) \\ 0 & \cdots & \cdots & \varphi(j_{m-1},j_m) & e(j_m) \end{bmatrix},$$

with

$$e(i)=-\lambda V_N(i)+E-2$$

and

$$\varphi(i_l,i_{l-1})=\begin{cases} 1 & \text{if } i_l=i_{l-1}+1 \\ 0 & \text{otherwise} . \end{cases}$$

B is a matrix most of whose elements are zero. B contains at most one nonzero element per row, whose value is 1. In these expressions the index m is $L/2$, which is just the degeneracy of the lowest-order result.

We now estimate the left-hand side of Eq. (27) and determine the energy eigenvalues to next order in λ^{-1}. Let us consider the energy eigenvalues which in lowest order are $\approx -\lambda$. These correspond to the matrix elements contained in submatrix A in (27). We want to compute possible splittings of this highly degenerate energy level. For values of $E \approx \lambda$, the diagonal elements in submatrix C are all of order λ, and so the largest contribution to the determinant in (27) will come from terms which multiply all these large diagonal elements. Thus for such values of E the leading contributions are given by solving

$$\text{Det}\begin{bmatrix} -\lambda+E-2 & \varphi(i_1,i_2) & \cdots & \cdots & 0 \\ \varphi(i_1,i_2) & -\lambda+E-2 & \cdots & \cdots & \vdots \\ \vdots & \vdots & & & \vdots \\ \vdots & \vdots & & & \varphi(i_{m-1},i_m) \\ 0 & \cdots & \cdots & \varphi(i_{m-1},i_m) & -\lambda+E-2 \end{bmatrix} (\lambda+E-2)^{N/2}=0$$

or

$$\text{Det}\begin{bmatrix} -\lambda+E-2 & \varphi(i_1,i_2) & \cdots & \cdots & 0 \\ \varphi(i_1,i_2) & -\lambda+E-2 & \cdots & \cdots & \vdots \\ \vdots & \vdots & & & \vdots \\ \vdots & \vdots & & & \varphi(i_{m-1},i_m) \\ 0 & \cdots & \cdots & \varphi(i_{m-1},i_m) & -\lambda+E-2 \end{bmatrix} =0 \ . \tag{28}$$

To evaluate (28), we need to determine the φ's. Each of the diagonal elements in (28) corresponds to a site of the chain for which $V_N(n)=+1$. From the construction of the Thue-Morse series, it is not difficult to see that $\frac{1}{3}$ of such sites are surrounded on both sides by sites at which the potential has a value $V_N(n)=-1$, while the remaining $\frac{2}{3}$ of the sites have one neighbor at which the potential has the value $V_N(n)=-1$. For pairs of neighboring sites with the same potential, $\varphi(i_{l-1},i_l)=1$, otherwise it is zero. Thus (28) reduces to

$$\text{Det}\begin{bmatrix} -\lambda+E-2 & 1 \\ 1 & -\lambda+E-2 \end{bmatrix}^{L/6} (-\lambda+E-2)^{L/6}=0 \ . \tag{29}$$

$L/6$ is thus the number of singlet sites with $V_N(n)=1$ as well as the number of nearest-neighbor pairs of sites with the same potential.

It is easy to solve (29) for the first-order energy eigenvalues. A similar equation holds for those energy eigenvalues that are close to $-\lambda$. The result is that to first order each of the two highly degenerate energy levels is split into three levels with energies

$$E=\lambda+2,\lambda+2\pm1,-\lambda+2,-\lambda+2\pm1 \ ,$$

each of which is $L/6$-fold degenerate. This lowest-order splitting is clearly due to the mixing among mutually degenerate states. Mixing between states whose energies are near λ and whose energies are near $-\lambda$ will occur in the next order in λ^{-1}.

There is a simple physical interpretation of this result. To understand how degeneracies are lifted, let us focus on particles sitting in a region of the chain in which the potential, $V_N(n)=-1$. Since, to this order, there is no mixing between localized states subject to different values of $V_N(n)$, the energies of those states which are confined to a unit interval such that both their neighboring intervals have $V_N(n)=1$, will be unaffected by the lowest-order nearest-neighbor mixing. The remaining $\frac{2}{3}$ of the states originally associated with the potential $V_N(n)=-1$ will have one neighboring interval with $V_N(n)=-1$. For those states which now see two neighboring regions of the chain with the same potential, the symmetric and antisymmetric linear combinations of the localized states are now the energy eigenstates. As usual, the energy of the symmetric combination will be lower than the unperturbed energy, while the antisymmetric combination will be higher, by the same amount. Thus $\frac{1}{3}$ of the states originally degenerate with energy $E=-\lambda$ will now occupy each of the three equally spaced energy levels into which this band has split, as a result of the nearest-neighbor perturbation. A similar argument applies to the breaking of the degeneracies between particles localized in regions of the chain with $V_N(n)=1$. We therefore obtain the six equally degenerate levels described above.

Figure 2 shows a plot of the tight-binding energy spectrum computed numerically from Eq. (26) with $N=8$ and $\lambda=5$, 1, 0.5, and 0.2. We see that in Figs. 2(a)–2(c), the largest gaps neatly divide the spectrum into six regions. These are the bands which in our first-order strong-perturbation approximation are degenerate. Notice that when the energies are arranged in increasing order, the gaps are equally spaced and divide the system into six regions. Let z be the Bloch index. We see that for very large coupling [Fig. 2(a)] the gap at $z=\frac{1}{2}$ is largest, while the gaps at $\frac{1}{6}$, $\frac{1}{3}$, $\frac{2}{3}$, and $\frac{5}{6}$ are smaller. We also observe that as λ decreases, the gap at $z=\frac{1}{2}$ shrinks faster than the gaps at $m/6$ ($m\neq3$). In Fig. 2(d) the gap at $z=\frac{1}{2}$ is almost gone, and the largest gap is at $z=\frac{2}{3}$, corresponding to the large peak in Fig. 1 at $k=\frac{1}{3}$, as predicted by Eq. (25).

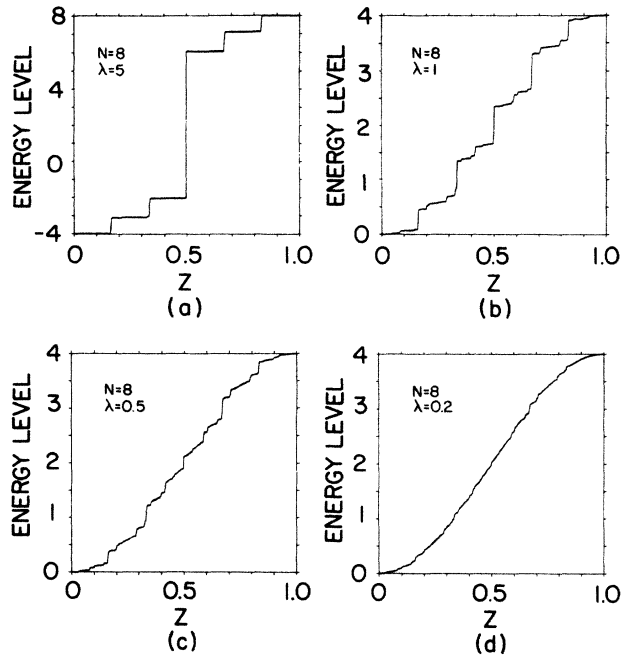

FIG. 2. Energy spectrum calculated from Eq. (26) for the Thue-Morse chain with $N=8$ for various values of λ. (a) $\lambda=5$, (b) $\lambda=1$, (c) $\lambda=0.5$, (d) $\lambda=0.2$.

The qualitative behavior of the gaps as a function of λ is easily understood. For the moment, let us consider only chains of finite length. (The $N\rightarrow\infty$ limit will be discussed below.) The gap at $z=\frac{1}{2}$ for large λ just reflects the simplest average symmetry of the Thue-Morse chain: Since half of the elements in the chain are of each type, half the highly localized states are associated with each of the two values of the potential. The gaps at $z=m/6$ ($m\neq 3$) are associated with sequences of single and double occurrences of the potential, as explained above. As λ decreases, the localization length becomes longer, and differences in the average potential seen by each state become smaller. The first property of the potential to "average out" is the most local one, namely the single-site potential. Thus the gap at $z=\frac{1}{2}$ disappears faster than other gaps which are associated with sequences of the potential extending over several lattice spacings. On the other hand, as λ decreases, wave functions will be able to distinguish between increasingly longer sequences, and so new gaps will open. These gaps, while smaller in magnitude, will diminish still more slowly as λ decreases.

At first sight, the origins of the gaps in the weak- and strong-coupling limits appear to be somewhat different. In the strong-coupling case, gaps appear at $z=m/6$ because all six energy states are equally degenerate. In weak coupling, on the other hand, there is a large gap at $z=\frac{2}{3}$ because there is a large peak in the structure factor at $k=\frac{1}{3}$, at least for a finite system. (For weak coupling, z is roughly twice the inverse wave length of the state.) In fact, however, the origin of the gaps in both limits is related. As we discussed earlier, the equal degeneracy of the six energy levels that appear in strong coupling is due to the fact that in the Thue-Morse chain, the sequence *aba* occurs exactly half as often ($\frac{1}{3}$ of the time there is a *b* in the chain), as the sequence *abba*. (Here *a* and *b* are associated with different value of the potential.) But a short sequence which repeats more or less uniformly throughout the chain with finite density will give rise to a peak in the structure factor at a k which is the inverse of its average repeat distance. Thus it is natural to expect peaks in the structure factor at values of $k=\frac{1}{2}$, $\frac{1}{6}$, and $\frac{1}{3}$, and using (25), corresponding gaps in the energy spectrum, even for small λ. We see, then, that although the Thue-Morse chain has a complicated and unusual symmetry, it is still the symmetry that determines the qualitative features of the spectrum for any value of λ, as in simple periodic systems.

C. The $N\rightarrow\infty$ limit

In Sec. III B we described the electronic spectrum of the finite Thue-Morse chain. We now want to consider the fate of the gaps in the $N\rightarrow\infty$ limit. In ordinary periodic and quasiperiodic systems, the peaks in the structure factor increase in intensity as the size of the system grows proportional to L^2. As a result, the determination of the positions of the gaps in the thermodynamic limit is often straightforward (although usually nontrivial). In the Thue-Morse system, on the other hand, the peaks in the structure factor scale with different exponents which are a function of k. Except for the trivial peak at $k=\frac{1}{2}$, which just represents the underlying periodicity associated with the unit length of the Thue-Morse potential, all the peaks scale with an exponent less than 2. Thus relative to the large peak at $k=\frac{1}{2}$, the structure factor looks more and more like that of an amorphous system as L increases, making a determination of the energy spectrum in the thermodynamic limit more difficult.

It is useful to see how this difficulty manifests itself in the context of weak-perturbation theory. The second-order perturbation-theory result displayed in Eq. (25) indicates that the gaps should disappear as $L\rightarrow\infty$ since $\tilde{V}_N(k)/L^2\rightarrow 0$ as $L\rightarrow\infty$. However, this argument is inadequate. As we stated earlier, the average unperturbed level separation decreases like L^{-1} while the size of the weak perturbation does not decrease that quickly. Thus as the system grows we must use near-degenerate perturbation theory with increasingly many nearly degenerate states to obtain reliable results. In addition, as L increases, more new peaks in the structure factor appear close to a given value of k, so that many more terms must be included in the perturbing potential. From the weak-coupling point of view, it is very difficult to analytically determine the band structure in the thermodynamic limit, even qualitatively.

In the context of the strong-perturbation approximation, the $L\rightarrow\infty$ limit is somewhat more straightforward. In this approach the gaps persist since the wave functions are more or less localized. If the system is much larger than the finite-localization length, any further increase in the size of the system is expected to have a negligible effect on the gaps. The following scenario thus suggests itself: As λ decreases for a finite system, the existing energy gaps decrease in magnitude, while new, smaller gaps

appear. If λ is fixed, the localization length is fixed, and increasing the system size well beyond the localization length will not substantially affect the sizes of the gaps. Thus as $N \rightarrow \infty$ for fixed λ, the gaps are expected to persist. In this regard the system is reminiscent of a random chain with diagonal disorder. Since gaps persist in that system in the thermodynamic limit, they will persist in our system *a fortiori,* so long as the localization length is finite. Notice that this is not what a naive application of second-order weak-perturbation theory [Eq. (25)] would suggest, since the intensities of all the nontrivial peaks scale with an exponent less than 2. But, as we argued earlier, nondegenerate perturbation theory is inapplicable in this limit in any case. Unfortunately, since we have no reliable analytic results for small λ and $N \rightarrow \infty$, we cannot completely rule out the existence of a transition at some finite λ to a state with no gaps. More work is needed to dispose of this possibility.

IV. SUMMARY

In this paper we have studied the structure factor and electronic properties of the Thue-Morse chain. Despite the simplicity of the algorithm by which it is generated, this system has a remarkably interesting structure, being neither periodic, quasiperiodic nor random. We found that the structure factor consists of a dense set of delta-function peaks, as in quasiperiodic systems. However, unlike quasiperiodic systems, the peaks in the spectrum scale with the size of the system in a complicated way. We have proved a number of general properties about these exponents, and in particular, we have shown that all the peaks scale with an exponent less than 2 and thus vanish relative to the peak at the center of the Brillouin zone as the system grows.

We have also described, semiquantitatively, the energy spectrum of the chain, in the context of a discrete tight-binding approach with both weak and strong potentials. We have qualitatively described the origin of the gaps in both limits and showed how they are related. Our arguments have also led us to conclude that for any fixed potential strength there are nonzero gaps in the limit of an infinite system. This conclusion is contrary to the expectations of naive nondegenerate perturbation theory, and, as we have discussed, is probably related to the appearance of additional small peaks in the structure factor as the size of the system increases. Because of the intrinsically hierarchical nature of the Thue-Morse algorithm, it should be possible to demonstrate these ideas more quantitatively using a renormalization group approach. We are currently working on this problem.

Finally, we note that we have fabricated and experimentally studied GaAs-AlAs Thue-Morse superlattices using molecular beam epitaxy techniques.[9] Because of their intriguing properties, physical realizations of systems which are not periodic, quasiperiodic, or random may be of significant experimental and technological interest.

ACKNOWLEDGMENTS

We are grateful to L. Sander for useful comments on the manuscript. This work was supported by the U.S. Department of Energy under Grant No. DE-FG02-85ER45189 and by the National Science Foundation under Grant No. DMR-8602675.

[1]B. Simon, Adv. Appl. Math. **3**, 463 (1982); J. Bellisard, D. Bessis, and P. Moussa, Phys. Rev. Lett. **49**, 701 (1982); M. Kohmoto, L. P. Kadanoff, and C. Tang, *ibid.* **50**, 1870 (1983); S. Ostlund, R. Pandit, D. Rand, H. J. Schellnhuber, and E. D. Siggia, *ibid.* **50**, 1873 (1983); S. Ostlund and R. Pandit, Phys. Rev. B **29**, 1394 (1984).

[2]J. P. Lu, T. Odagaki, and J. L. Birman, Phys. Rev. B **33**, 4809 (1986); Q. Niu and F. Nori, Phys. Rev. Lett. **57**, 2057 (1986); M. Kohmoto, Phys. Rev. B **34**, 5043 (1986); M. Kohmoto, B. Sutherland, and C. Tang, *ibid.* **35**, 1020 (1987); M. Fujita and K. Machida, J. Phys. Soc. Jpn. **56**, 1470 (1987); S. Aubry, C. Godreche, and F. Vallet, J. Phys. (Paris) **48**, 327 (1987); J. B. Sokoloff, Phys. Rev. Lett. **58**, 2267 (1987); T. Schneider, A. Politi, and D. Wurtz, Z. Phys. B **66**, 469 (1987).

[3]D. Schectman, J. Blech, D. Gratias, and J. W. Cahn, Phys. Rev. Lett. **53**, 1951 (1984).

[4]P. Levine and P. J. Steinhardt, Phys. Rev. Lett. **53**, 2477 (1984).

[5]R. Merlin, K. Bajema, R. Clarke, F.-T. Juang, and P. K. Bhattacharya, Phys. Rev. Lett. **55**, 2915 (1985).

[6]F. Axel, J. P. Allouche, M. Kleman, M. Mendes-France, and J. Peyriere, J. Phys. C **47**, 181 (1986).

[7]M. Kac, Ann. Math. **47**, 33 (1946).

[8]The weak-perturbation calculations of Sec. III A could just as easily have been carried in the context of the continuum Schrödinger equation of which (22) is a discrete version. However, the strong-coupling calculations of III B require a short-distance cutoff and cannot be performed in a straightforward way in the context of the continuum equation. For purposes of clarity, we have chosen to always work in the context of the tight-binding theory, but the direct applicability of the weak-perturbation results to the continuum theory should be borne in mind. More generally, the qualitative features of energy spectrum which we deduce should apply also to the continuum theory, since the symmetry of the potential is the same.

[9]R. Merlin, K. Bajema, J. Nagle, and K. Ploog, in Proceedings of the Third International Conference on Modulated Semiconductor Structures, Montpellier, France, 1987 [J. Phys. (Paris) (to be published)]; R. Merlin, Z. Cheng, R. Savit, J. Nagle, and K. Ploog (unpublished).